microbiology research

MDPI

Article

Studying the Anti-Virulence Activity of Meta-Bromo-Thiolactone against *Staphylococcus aureus* and MRSA Phenotypes

Rihaf Alfaraj [1,*], Esra K. Eltayb [1], Bashayer M. AlFayez [1], Amjad Abohamad [1], Eram Eltahir [1], Naifa A. Alenazi [1], Sandra Hababah [1], Hamad Alkahtani [2], Thamer A. Almangour [3], Fulwah Y. Alqahtani [1] and Fadilah S. Aleanizy [1]

[1] Department of Pharmaceutics, College of Pharmacy, King Saud University, Riyadh 11495, Saudi Arabia; fyalqahtani@ksu.edu.sa (F.Y.A.); faleanizy@ksu.edu.sa (F.S.A.)
[2] Department of Pharmaceutical Chemistry, College of Pharmacy, King Saud University, Riyadh 45142, Saudi Arabia; ahamad@ksu.edu.sa
[3] Department of Clinical Pharmacy, College of Pharmacy, King Saud University, Riyadh 11495, Saudi Arabia; talmangour@ksu.edu.sa
* Correspondence: ralfaraj@ksu.edu.sa

Abstract: Quorum-sensing inhibitors have recently garnered great interest, as they reduce bacterial virulence, lower the probability of resistance, and inhibit infections. In this work, meta-bromo-thiolactone (mBTL), a potent quorum and virulence inhibitor of *Staphylococcus aureus (S. aureus)* and methicillin-resistant *S. aureus* (MRSA), was formulated in chitosan nanoparticles (ChNPs) using the ionic gelation method. The mBTL-loaded-ChNPs were characterized by their particle size, polydispersity index, zeta potential, morphology, and drug release profile. The results show that the mBTL-loaded-CNPs comprised homogenized, spherical nanoparticles ranging from 158 ± 1.3 to 284 ± 5.6 nm with a sustainable release profile over 48 h at 37 °C. These findings confirm the successful preparation of mBTL-loaded-ChNPs. Confocal laser scanning microscopy showed a significant reduction in the number of viable cells, indicating the antibacterial efficacy of mBTL. Biofilms were observed by scanning electron microscopy, which showed that the bacterial cells in the control experiment were enclosed in thick biofilms. In the presence of mBTL, the bacterial cells remained disordered and did not form a biofilm. mBTL-loaded-ChNPs represent a potential approach to overcoming antimicrobial resistance in the treatment of MRSA infection.

Keywords: *Staphylococcus aureus*; MRSA; mBTL; mBTL-ChNPs; antibiotic resistance; quorum sensing; virulence; biofilm

Citation: Alfaraj, R.; Eltayb, E.K.; AlFayez, B.M.; Abohamad, A.; Eltahir, E.; Alenazi, N.A.; Hababah, S.; Alkahtani, H.; Almangour, T.A.; Alqahtani, F.Y.; et al. Studying the Anti-Virulence Activity of Meta-Bromo-Thiolactone against *Staphylococcus aureus* and MRSA Phenotypes. *Microbiol. Res.* **2023**, *14*, 1596–1609. https://doi.org/10.3390/microbiolres14040110

Academic Editors: Niels Frimodt-Møller and Luca Grispoldi

Received: 27 August 2023
Revised: 29 September 2023
Accepted: 4 October 2023
Published: 10 October 2023

1. Introduction

Methicillin-resistant *Staphylococcus aureus* (MRSA) refers to a bacterium that is resistant to many available antibiotics, including β-lactam. MRSA is the predominant pathogen contributing to antimicrobial resistance (AMR) in both community and healthcare settings. Studies have shown that 33% of people carry *S. aureus* in their nose without harm, and 2% of these individuals are MRSA carriers [1]. The consequences of MRSA infection continue to surge because of elevated transmission rates, high rates of colonization, and rapid bacterial activation of virulence factors that increase pathogenicity. Bacterial population expansion is regulated by quorum sensing (QS), which is a form of intercellular communication [2]. In *S. aureus*, the quorum-sensing accessory gene regulator (*agr*) system controls virulence factor production. *Agr* is activated at a high cell density and triggers the secretion of auto-inducing peptides (AIPs), which are detected by transmembrane receptors that activate the bacterial virulence factors that drive infection. *S. aureus* pathogenicity is highly dependent on virulence factors, which include toxins (hemolysins), immune-evasive surface factors

(capsule and protein A), and biofilm formation [3]. *S. aureus* has two QS systems encoded by the *agr* locus; RNAII originates from the P2 promoter, and RNAIII originates from the P3 promoter. The RNAIII segment of *agr* includes *agrA*, *B*, *C*, and *D*, which encode the main components of the QS system. The transmembrane protein AgrB mediates AIP signal secretion, modification, and AgrD processing. The *agrA* gene encodes the cytosolic response regulator (RR), and *agrC* encodes a membrane-bound histidine kinase (HK). Together, they form a two-component regulatory system (AgrAC TCS) [4]. The ideal antibiotic for MRSA does not yet exist, but such an agent should have the following properties: rapid bactericidal killing; excellent tissue penetration; consistent pharmacokinetics and pharmacodynamics that allow for predictable dosing; low potential for the development of resistance while on therapy; low side effect profile; and demonstrated clinical and microbiological efficacy. As such an agent is not currently available, some have advocated combination therapy to fill in the gaps where each individual agent fails. Until recently, goals of combination antibiotic therapy have included maximizing bacterial clearance, preventing emergence of resistance and ensuring delivery of adequate drug to sites of infection. However, with recent studies suggesting there may be increased toxin release and subsequent host inflammation in infections caused by CA-MRSA clones, 9, 10 an additional benefit of combination therapy against CA-MRSA may be attenuation of toxin production as anti-virulence agents [5]. Synthetic molecules of meta-bromo-thiolactone (mBTL) strongly inhibit virulent bacterial QS and provided the uppermost activity for QS system inhibition against gram-negative bacteria such as *Pseudomonas aureginosa* [6]. The regulatory effect of mBTL molecules on Quorum Sensing (QS) is mediated by their disruption of intercellular communication among bacteria. It is probable that these molecules interfere with the signaling pathways through their binding to essential components of quorum sensing (QS), such as signal molecules or receptors [7]. Consequently, this binding activity hinders the coordination of bacterial actions, including the generation of virulence factors or the creation of biofilms [8].

mBTL molecules can be used to regulate the QS and may represent an alternative to traditional antibiotic therapy and an approach to reduce multi drug resistance (MDR). The therapeutic index of pharmacological agents can be increased by achieving sustained drug release via polymeric nanoparticles [9]. Also, mBTL is hydrophobic with low solubility and absorption so to increase its solubility and in accordance absorption it is subjected to nanoformulation. Chitosan is a class of polymers derived from chitin, a natural polysaccharide comprised of-(1,4)-linked N-acetyl glucosamine units. Fungi and the exoskeletons of crustaceans and insects are the most prevalent sources of chitin [10]. Chitosan-based nanoparticles can be used to deliver active components, such as pharmaceuticals or natural products, via several modes of administration. Chitosan nanoparticles combine the unique characteristics of a polymer with tunable size and the capacity to modify the surface to meet specific requirements, making them a very promising and diverse solution for overcoming the bioavailability and stability difficulties that affect most active ingredients [10]. The aim of this work was to formulate mBTL in chitosan nanoparticles and test their effect on gram-positive bacteria such as *S. aureus*, MRSA, and biofilm formation in a series of QS mutants that might demonstrate various levels of virulence. Agr mutants are of significant importance in the field of an-ti-quorum sensing (anti-QS) research, specifically in relation to *Staphylococcus aureus* and other Gram-positive bacteria. The utilization of Agr mutants in anti-quorum sensing (QS) investigations is justified by the following reasons: The validation of the Agr system as a target for anti-quorum sensing (QS) chemicals is facilitated by the utilization of Agr mutants. Through the examination of mutations in this particular system, scientists have verified that the inhibition or modulation of Agr can disrupt behaviors regulated by quorum sensing (QS) [11]. Controlled experiments can be conducted using Agr mutants to assess the effectiveness of prospective anti-quorum sensing (QS) compounds. To comprehend the specificity of these chemicals, a comparative analysis of their impact on wild-type strains, which possess intact Agr systems, and Agr mutants [12].

The use of Agr mutants enables researchers to acquire more profound understanding of the mechanisms underlying the effectiveness of anti-quorum sensing (QS) drugs, as well as their potential as novel approaches for addressing bacterial infections.

2. Materials and Methods

2.1. Bacterial Strains, Chemicals, and Growth Conditions

Strains of *S. aureus*, MRSA, and different QS mutants (Table 1) were cultured in tryptic soy broth (TSB) and tryptic soy agar (TSA) supplemented with erythromycin and incubated at 37 °C for 18–24 h [13].

Table 1. Description of *Staphylococcus aureus* strains in this study.

Strain Name	Abbreviation	Description
Staphylococcus aureus	*S. aureus*	Wild-type
Methicillin resistant Staphylococcus aureus	MRSA	Methicillin-resistant *Staphylococcus aureus*
NE1532	AgrA	4 P16 *agrA* accessory gene regulator protein A SAUSA300_1992
NE95	AgrB	1 O21 *agrB* accessory gene regulator protein B SAUSA300_1989
NE873	AgrC	3 B17 *agrC* accessory gene regulator protein C SAUSA300_1991

2.2. Preparation of Chitosan Nanoparticles (ChNPs) and mBTL Loading

ChNPs were prepared using the ionic gelation method [14] by dissolving ten mL of 1% *v/v* acetic acid in 100 mL of deionized water, and then 100 mg of chitosan was added and magnetically stirred for two–three h until it was completely dissolved. The nanoparticles could be affected by the acidic media; accordingly, the solution pH was adjusted using sodium hydroxide (NaOH) to a pH of 4.7. mBTL 4% was dissolved in 1200 µL of dimethylsulphoxide (DMSO) and 1000 µL of tween 20, and the resulting mixture was then added to the prepared chitosan solution. To 10 mL of chitosan solution containing the drug, DMSO, and tween 20, four mL of 0.01% *w/v* tripolyphosphate (TPP) solution was added. This mixture was then continuously magnetically stirred at 500 rpm for 30 min. The nanoparticles were formed. The nanoparticle solution was then centrifuged twice at 14,000 rpm for 30 min using a cooling centrifuge. The retrieved nanoparticles were then suspended in deionized water. Finally, the ChNPs were reconstituted in deionized water and stored at 4 °C for further characterization.

2.3. Physicochemical Analysis of mBTL-Loaded ChNPs

The mean particle size, polydispersity index, and zeta potential of the mBTL-ChNPs were measured at 25 °C using the Zetasizer Nano ZS (Malvern Instruments, Malvern, UK). The nanoparticle suspension was diluted five times with deionized water. All measurements were performed in triplicate.

2.4. Determination of mBTL-Loaded ChNP Encapsulation Efficiency (EE%)

The encapsulation efficiency of the mBTL-ChNPs was indirectly determined by measuring the concentration of free mBTL in the aqueous phase. The encapsulation efficiency was estimated using the following equation:

$$\%\text{Entrapment Efficiency} = \frac{\text{total amount of drug loaded} - \text{free drug in supernatant}}{\text{total amount of drug loaded}} \times 100 \quad (1)$$

2.5. In Vitro Release of mBTL-ChNPs

The release profiles of mBTL-ChNPs were evaluated by means of the dialysis method using a cellulose dialysis tube sealed at both ends. The membrane was soaked in a release medium overnight before use. Then, 1 mL of mBTL-ChNPs was placed into dialysis bags, which were then transferred into beakers containing 30 mL of the phosphate buffer pH 7.4.

At predetermined time intervals of 0.5, 1, 2, 4, 5, 6, 7, 8, 24, and 48 h. Three mL of the release medium was withdrawn and instantly replaced with an equal amount of fresh release medium to maintain a sink condition. The amount of released mBTL was determined by measuring the absorbance at 280 nm. The release profile of the mBTL was obtained by plotting the cumulative percentage release of the drug versus time.

2.6. Growth Curve Construction

All bacterial strains were grown in 5 mL of TS broth with the selected antibiotic marker erythromycin except for the fourth wild-type strain, and then incubated at 37 °C with continuous overnight shaking at 200 rpm. Thereafter, 200 µL of bacterial broth with an optical density (OD) of 0.4–0.6 McFarland was added to 96-well plates. All tests were performed in triplicate with controls of media only and untreated bacteria. Then, the 96 well plates were placed in the BioscreenC reader, and the optical density of the bacterial growth was recorded at 600 nm for 24 h.

2.7. MIC Measurements

According to the (Clinical & Laboratory Standards Institute) CLSI guidelines, the minimal bactericidal concentration (MBC) is defined as the first dilution that results in three or fewer colonies after 24 h of incubation at 37 °C. The double-dilution method [14,15] is the standard method for determining minimal inhibitory concentrations (MICs). The minimal inhibitory concentrations were determined by measuring the concentration of the formula at which no visible growth occurred. The minimal bactericidal concentration (MBC) was also recorded as the lowest concentration of the compound at which no colonies formed after plating the dilutions around the MIC or growing them in fresh TSB media. For all strains, the MBCs were determined by the inoculation of ten µL from each well that did not show visible bacterial growth on the TS plates. After 24 h of incubation at 37 °C, the first dilution that yielded three colonies or fewer was scored as the MBC, as described by the CLSI.

2.8. Hemolytic Activity Analysis

For hemolytic activity analysis, an overnight culture of all strains was standardized to an OD_{600} of 0.5 and 1:50 diluted in ten mL TSB with or without antibiotic and tested formula. The strains were streaked on blood agar plates and incubated overnight at 37 °C for 24 and 48 h. The hemolytic activity was observed on plates as transparency around the colonies [10].

2.9. Biofilm Assay

Modifications were made to the method previously described for detecting biofilms [16]. The strains were cultivated at 37 °C for 24 h in TSB broth, diluted to 107 cfu/mL in TSB media, and dispensed in 96-well microliter plates (Thomas Science, Chadds Ford, PA, USA). Then, 100 µL of each antibiotic and compound at 1 mg/mL FC were added to each well. Biofilm inhibition was evaluated by inoculating 15-well plates with each strain (100 µL of bacterial strain was added to each well) and incubating the plates at 37 °C for 24 h. After removing the cell suspension, the plates were washed twice with a 0.9% sodium chloride (NaCl) solution and air-dried at room temperature for 1 h. After 15 min, the wells were stained with 150 µL of crystal violet solution (CV; Prolab Diagnostics, Richmond Hill, ON, Canada). Following the staining, the CV was removed, and 0.9% NaCl solution was used to wash the wells three times. The attached CV was dissolved in 200 µL of ethanol–acetone (80:20 v/v). Finally, a microplate reader was used to measure the CV absorbance at 595 nm (BioTek, Winooski, VT, USA). All experiments were carried out in triplicate for three independent times.

2.10. Confocal Microscopy

All strains were cultured in tryptic soy agar (TS) or TS agar supplemented with 10 mg/mL erythromycin at 37 °C for 18 h. Culture media were purchased from Oxoid (Basingstoke, Hampshire, UK). The cultures were treated with 0.5 mg/mL free mBTL, stained with Live/Dead BacLight viability stains (Syto 9 and propidium iodide (PI)), and then observed by CLSM (Leica TCS SP5, Weltzer, Germany. Images were acquired using Leica Application Suite Advanced Fluorescence software, version 5 (Leica, Weltzer, Germany), with an optical magnification of 40× using an oil-immersion objective lens. The images were sized to 1024 × 1024 pixels and recorded by scanning lasers over an area of 25 × 25 µm. An argon-based laser was employed for excitation at 488 nm, and a HeNe laser for excitation at 543 nm. The emission was set at 528 nm for SYTO 9 and 645 nm for PI. Via sequential scanning, the images were obtained and processed in Image J.

2.11. Scanning Electron Microscopy (SEM)

To visualize the biofilm formation, bacteria were grown overnight in TSB at 37 °C, then diluted in LB to 10^7 cfu/mL. Polyvinyl (Fisher Scientific, Hampton, NH, USA) coverslips were placed in each well of a 6-well plate, and then 2 mL of LB and 2 mL of diluted culture were added. Biofilms formed on the coverslips over 24 h at 37 °C, and then fixed with 3% glutaraldehyde in phosphate buffer, pH 7.2, for 24 h. After three washes with phosphate buffer, the coverslips were postfixed for 1 h with 1% osmium tetroxide (in H_2O), and then dried in an ethanol dehydration series (50, 60, 70, 80, 90, and 2 × 100% (*v*/*v*)) for 5 min at each concentration [17]. All samples were dried for 1 day and sputter-coated with a palladium-gold thin film. SEM/EDS imaging was performed in high-vacuum mode at 20 kV using an FEI Quanta 400FEG ESEM/EDAX Genesis X4M (FEI Company, Hillsboro, OR, USA).

3. Results

3.1. Nanoparticle Characterization

The average particle size, polydispersity index (PDI), and zeta potential were investigated. The particle size was 158.5 ± 1.3 nm and 283.9 ± 13.55 nm for blank ChNPs and mBTL-ChNPs, respectively, well below the 500 nm threshold to be considered nano-sized [9,10]. PDI values were ≤0.3, indicating the formation of a homogenous preparation. The zeta potential of the chitosan nanoparticles was positively charged, indicating good physical stability of the nano-preparations (Table 2). The morphology of the ChNPs was determined by TEM (Figure 1).

Table 2. Nanoparticle characteristics. Data represent means ± SD.

	Blank ChNPs	**mBTL-ChNPs**
Particle size (nm)	158.5 ± 1.3	283.9 ± 13.55
PDI	0.327 ± 0.016	0.253 ± 0.018
Zeta potential (Mv)	33.8 ± 0.361	19.6 ± 1.25

3.2. Encapsulation Efficacy of mBTL-ChNPs

The encapsulation of mBTL in the ChNPs was determined by assessing the encapsulation efficiency (EE%) and validated against a calibration curve of mBTL. The percentage of fresh mBTL encapsulated inside the ChNPs was 70.358%.

3.3. In Vitro Drug Release

The in vitro release of mBTL in 30 mL of phosphate buffer, pH 7.4, was evaluated over 24 and 48 h using a cellulose dialysis tube sealed at both ends. The release profile of mBTL was obtained by plotting the cumulative percent release of mBTL versus time (Figure 2).

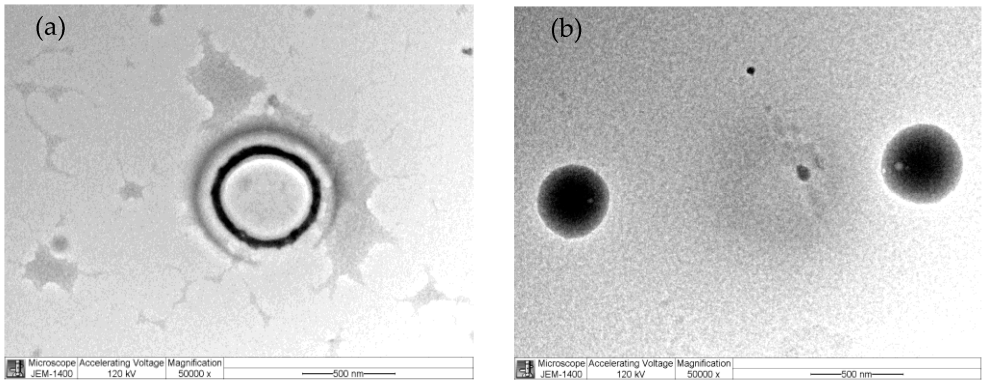

Figure 1. TEM images: (**a**) blank ChNPs and (**b**) mBTL-loaded ChNPs.

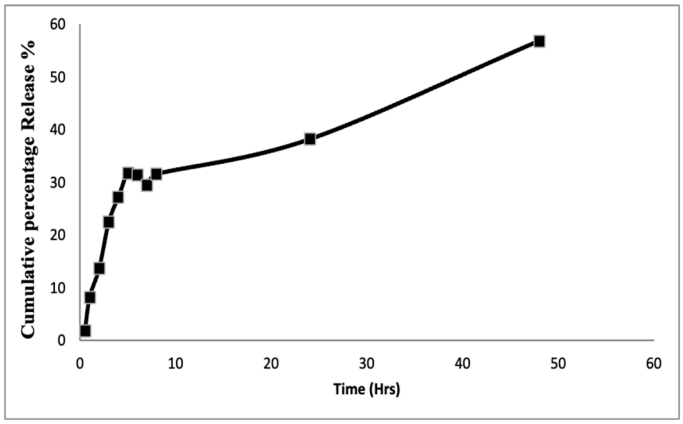

Figure 2. In vitro release profile of free mBTL.

3.4. Growth of S. aureus and Targeted Mutants in the Presence and Absence of mBTL and mBTL-ChNPs

The effects of mBTL, mBTL-ChNPs, and ChNPs were investigated in wild-type *S. aureus*, MRSA, and QS mutants NE1532 (AgrA), NE95 (AgrB), and NE873 (AgrC). Oxacillin was used as a positive control. Testing was performed at 2 mg/mL, 1 mg/mL, and 0.5 mg/mL mBTL (Figure 3). The growth of all strains was similar to their growth in the presence of empty ChNPs, demonstrating that the ChNPs were cytocompatible and had no bactericidal effect.

In the presence of mBTL-ChNPs, the growth of all strains was reduced significantly ($p < 0.05$), with reductions of 60.83% (wild-type), 98.76% (MRSA), and 100% in all QS mutant strains. mBTL alone produced a growth reduction in all strains; however, when loaded in ChNPs, its uptake increased and produced an enhanced killing effect.

Concentrations ranging from 2 mg/mL to 0.125 mg/mL in the free mBTL and mBTL-ChNPs were evaluated for antimicrobial activity based on MIC50 using the broth dilution method. A dose-dependent mBTL effect was observed, with 2 and 1 mg/mL producing a 100% killing effect. The MIC_{50} was 0.5 mg/mL for mBTL-ChNPs, while the MIC50 was 0.8 mg/mL for free mBTL and this concentration was chosen for further analysis. All experiments were carried out in triplicates and *t*-test were used for analysis.

3.5. Biofilm Inhibition by mBTL-ChNPs

The antivirulence effect of the mBTL-ChNPs in the context of biofilm formation was investigated in wild-type *S. aureus*, MRSA, and the QS mutants (Figure 4). The results show reductions of 51.7% (wild-type) and 50% (MRSA) versus 68% (NE1532/AgrA) and 63.6% (NE95/AgrB), and a significant reduction of 97.3% for NE873/AgrC ($p < 0.05$) (Figure 4).

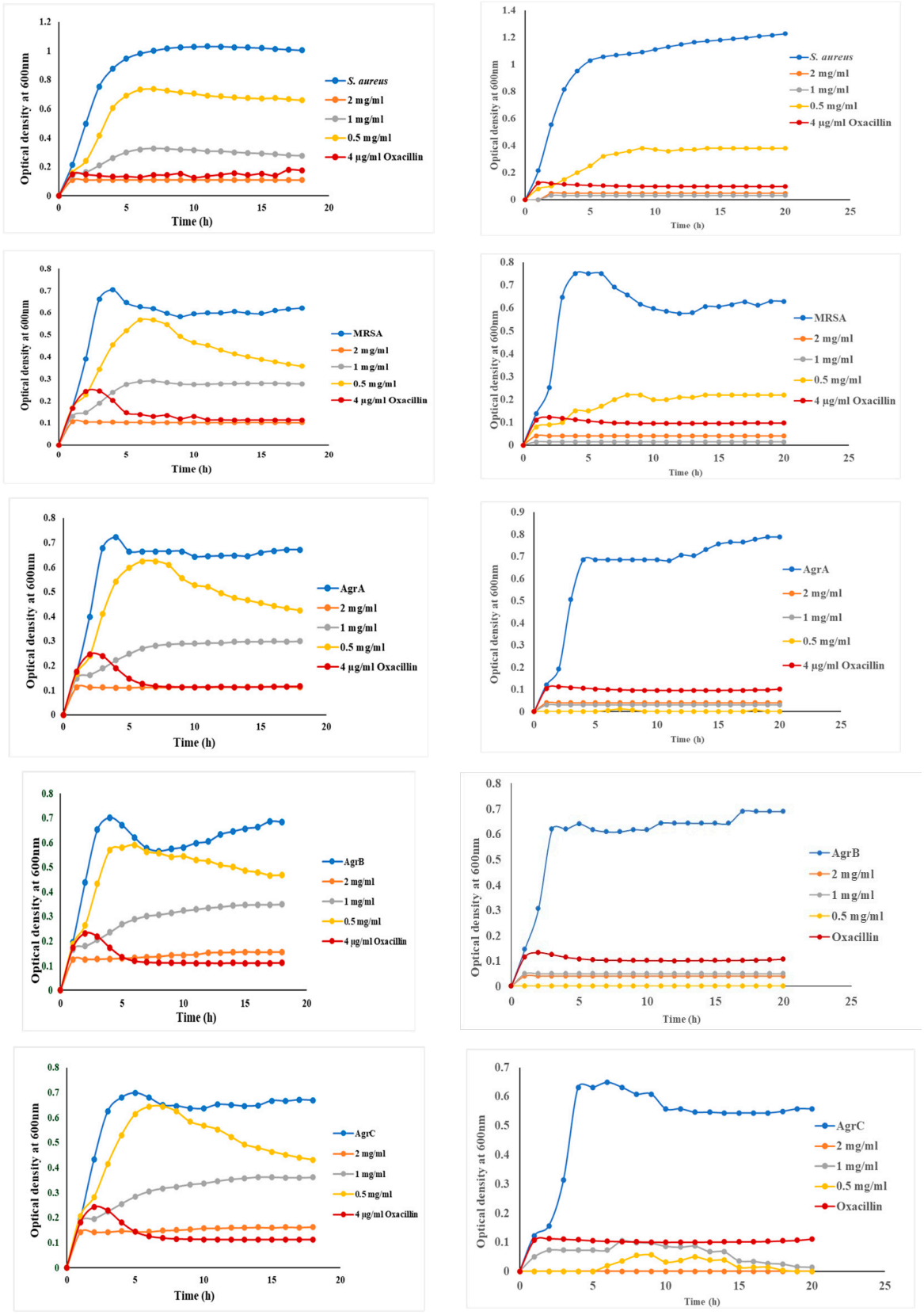

Figure 3. The effects of free mBTL (**a**) and mBTL-loaded-ChNPs (**b**) on bacterial growth of wild-type *S. aureus*, MRSA, and QS mutants NE1532 (AgrA), NE95 (AgrB), and NE873 (AgrC). All experiments were performed three times in triplicate.

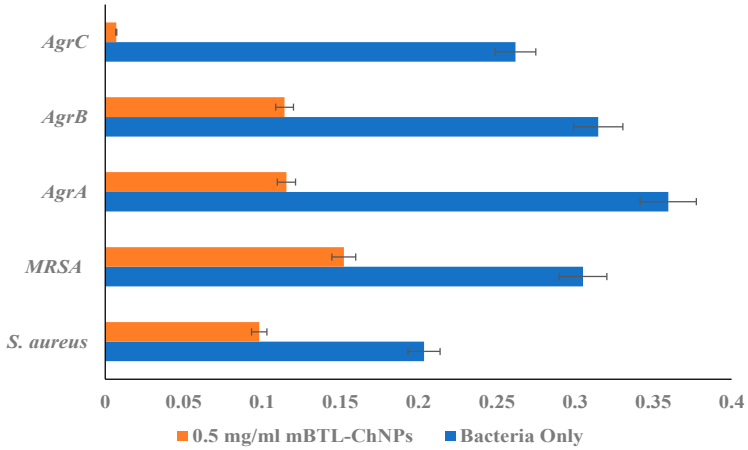

Figure 4. Inhibition of biofilm formation by mBTL-ChNPs in wild-type *Staphylococcus aureus*, MRSA, and QS mutants NE1532 (AgrA), NE95 (AgrB), and NE873 (AgrC).

3.6. Bacterial Viability in Biofilms Exposed to mBTL-ChNPs

Biofilms were live/dead-stained and observed by confocal laser scanning microscopy (CLSM) to determine whether the mBTL-ChNPs were capable of killing *S. aureus* in them (Figure 5). The majority of cells were alive in the control (untreated) biofilms (Figure 5a). On the other hand, the biofilms treated with 0.5 mg/mL mBTL-ChNPs showed an increase in the number of dead cells throughout the biofilm structure (Figure 5b–f). These findings demonstrate the significant killing effect of mBTL-ChNPs in already established biofilms.

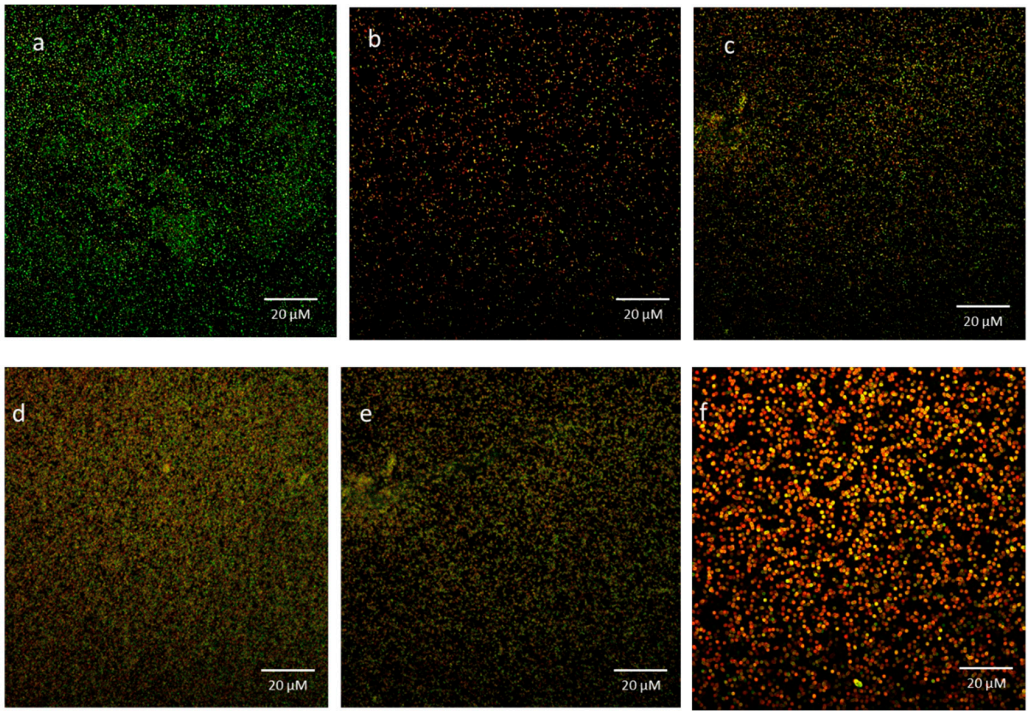

Figure 5. CLSM of Baclight Live/Dead (Syto-9 and PI)-stained biofilms in the absence and presence of mBTL-ChNPs. (**a**) Control cells in the absence of mBTL, green indicates 98% living cells; (**b**–**e**) cells treated with mBTL-ChNPs showed varying levels of cell death (red/yellow) and morphological changes; (**f**) over time, 92% cell killing was achieved.

3.7. SEM Imaging of Biofilms Treated with mBTL-ChNPs

The bacterial morphology in the biofilms formed after exposure to mBTL-ChNPs was investigated using SEM (Figure 6). Untreated *S. aureus*, MRSA, and the *AgrA*, *AgrB*, and

AgrC mutants formed biofilms (Figure 6a–e) that were disrupted by 0.5 mg/mL mBTL-ChNPs (Figure 6f–j).

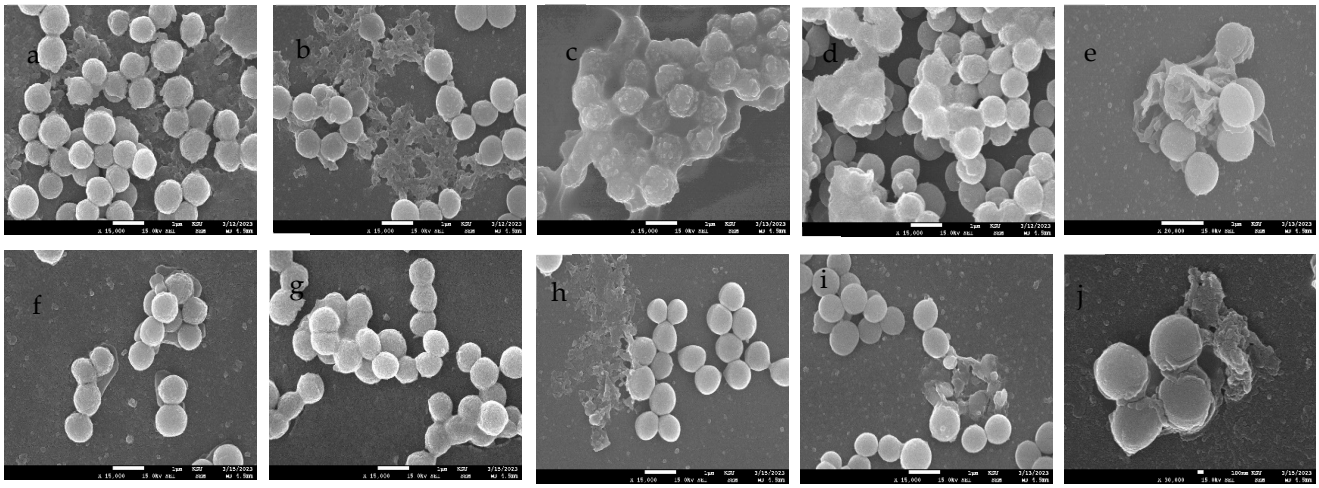

Figure 6. Scanning electron microscopy (SEM) images of (**a**) untreated *S. aureus*: spherical cells appearing as clusters, biofilms appearing as a dense extracellular matrix surrounding the cells; (**b**) untreated methicillin-resistant *staphylococcus aureus* (MRSA) cells: biofilm matrix appearing as a dense network of fibers surrounding the MRSA cells and connecting them; (**c**) untreated AgrA mutant cells showing altered cell morphology; the cells appear irregular, with a changed surface structure that appears as a capsule; (**d**) untreated AgrB mutant cells, with a thick biofilm (white shadow) and more surrounding bacterial cells; (**e**) untreated AgrC mutant cells; the biofilm appears more densely packed around the bacterial cells; (**f**) *S. aureus* cells treated with loaded mBTL-CNPs; the bacterial cells are separate from each other and lack a visible extracellular matrix; (**g**) MRSA cells treated with loaded mBTL-CNPs, lacking a visible extracellular matrix; (**h**) AgrA mutant cells treated with loaded mBTL-CNPs, exhibiting disorganized separation of biofilm from the cells; (**i**) Agr B mutant cells treated with loaded mBTL-CNPs without the thick biofilm seen in the control; (**d**) with more bacterial cells visible; (**j**) Agr C mutant cells treated with loaded mBTL-CNPs, exhibiting irregular arrangement of biofilm.

3.8. Hemolytic Activity of mBTL-ChNPs on S. aureus Strains

The hemolysis zones of all bacterial strains that were subjected to treatment with mBTL-loaded ChNPs were assessed on blood agar plates. The findings are illus-trated in Figure 7. As depicted in Figure 7, the hemolytic activity of untreated *Staphylococcus aureus*, methicillin-resistant *Staphylococcus aureus* (MRSA), and cells with mutations in AgrA, AgrB, and AgrC exhibited a similar level of hemoly-sis compared to bacteria treated with Chitosan nanoparticles loaded with mBTL. This observation indicates that there is no discernible and significant distinction between these conditions.

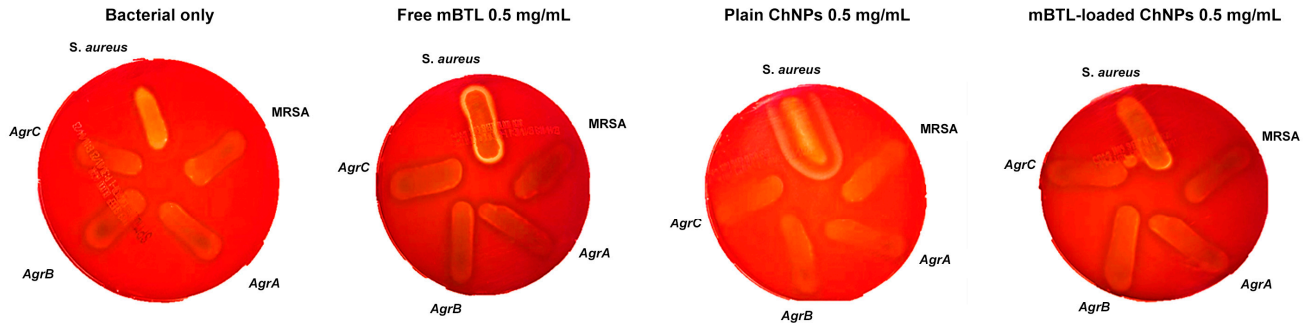

Figure 7. Hemolytic activity of *S. aureus*; MRSA; and the AgrA, AgrB, and AgrC mutants.

4. Discussion

Gram-positive *S. aureus* is exceptionally adaptable and flexible. It is a harmless commensal that resides on the skin and in mucous membranes [18]. However, it is also one of the top causes of hospital- and community-acquired infections globally because of its ability to grow in numerous tissues and circulate, causing significant diseases [19,20]. It can trigger several infections, ranging from simple skin infections to more serious systemic infections that can even be fatal, such as pneumonia, osteomyelitis, and endocarditis. *S. aureus* infections recur in 8–33% of all cases, leading to significant human morbidity and mortality [21]. MRSA can cause skin or blood infection. MRSA spreads through contact with medical personnel and can result in various unpleasant complications, such as pneumonia, bacteremia, and surgical site infections. In contrast, community-associated MRSA (C-MRA) leads to skin and soft tissue infections among those who have never had contact with a healthcare setting. Despite this, MRSA infections continue to be the leading cause of increased mortality, healthcare expenses, and lengthened hospital stays [22]. The use of anti-QS molecules, such as mBTL, is one of the approaches used for targeting microbial virulence, as reported previously. Previous studies performed in our lab revealed the antimicrobial and antibiofilm activity of mBTL-calcium alginate NPs against different Pseudomonas isolates. It is curious that mBTL, our most potent in vivo inhibitor, is a partial ago-nist/partial antagonist of gene in the recombinant s. aureus. This feature of mBTL may be critical for its ability to function in vivo. Because specific gene act recipro-cally to control key virulence genes. Therefore, this study aimed to formulate mBTL in CNPs and evaluate their antimicrobial and antibiofilm activity.

In agreement with previous studies [23,24], plain nanoparticles and mBTL-loaded chitosan nanoparticles were synthesized with particle sizes of 158 $\pm$ 1.3 nm and 283.9 $\pm$ 13.55 nm, respectively, and a positive surface charge. This made it easy for these nanoparticles to be taken up by *S. aureus* and other strains due to the negative charge of the organisms.

Microbiological examination and comparison with free mBTL were conducted on mBTL-loaded CNPs. The AIP antagonist activity can be observed through substitution, truncation, or even a combination of these modifications of the native AIP. mBTL is a synthetic analog of Acyl-HSL. Other synthetic analogs have been tested for quorum-sensing inhibition in *S. aureus*; these compounds exert their action through the noncompetitive inhibition of AIP by altering its activation efficacy; they may also act as an allosteric inhibitor of Agr C [25,26].

The selected concentrations of mBTL were 2 mg/mL, 1 mg/mL, and 0.5 mg/mL. A greater effect on the different strains of *S. aureus* was observed at 2 mg/mL of mBTL. Furthermore, the findings of this study revealed that mBTL inhibited the growth of wild-type *S. aureus*, MRSA, and other QS mutants. Interestingly, the optical density presented in the growth curves of mBTL-loaded ChNPs was subtracted from the optical density of ChNPs alone, indicating that this antibacterial activity was enhanced after ChNPs were loaded with mBTL, as shown in the growth curves. The superior inhibition of bacterial growth exhibited by loaded mBTL compared to the free mBTL was in agreement with the results of other studies [27].

A biofilm is a type of microbial community that has adapted to living in various habitats, such as on human skin and medical equipment. They are responsible for two-thirds of all infections and also pose a significant risk in medical and industrial settings [28]. Infections by biofilm-forming microorganisms are notoriously difficult to treat because they exhibit a form of multidrug resistance called adaptive multidrug resistance [28]. Conventional antibiotics fail to eradicate biofilms because of several causes. Antibiotic resistance is multifaceted, encompassing biofilm formation, adaptive stress responses, and metabolic inactivation due to nutrition and gas limitations [29].

Gram-positive bacterial QS systems have peptide autoinducers that are encoded in the genome, thus allowing for the creation of peptides specific to each species. The Gram-positive opportunistic bacterium *Staphylococcus aureus* is responsible for nosocomial illnesses, such as sepsis and pneumonia [30]. MRSA and other *S. aureus* strains resistant to

various B -lactam antibiotics are on the rise. Virulence is regulated by the QS system, which is the accessory gene regulator (*agr*). The RNAII and RNAIII transcripts are transcribed by the P2 and P3 promoters. To regulate the feed-forward loop for quorum-sensing autoinducer peptide expression, a transcript encoding the *agrBDCA* locus is required. In *S. aureus*, the QS system is required for gene expression and to escape the immune system and establish an infection. The system is encoded by the chromosomal locus called the accessory gene regulator (*agr*). The locus comprises two operons produced by the P2 and P3 promoters. The P2 promoter encodes *agrBDCA* and controls the RNAII transcript, whereas the P3 promoter controls the RNAIII transcription, considered the effector molecule of the *agr* locus. The communication within the cells is regulated by AIP, which comprises a thiolactone ring synthesized by the condensation of the carboxyl group in the C-terminus and the sulfhydryl group in the cysteine. This process results in a structure that is necessary for binding the AIP to its receptor AgrC [30].

AIP is translated as an AgrD precursor. Then, the transmembrane protein AgrB converts it into a mature AIP and transports the peptide outside the cell. When additional bacterial cells are present, the AIP accumulates and binds to AgrC, a membrane-bound histidine-kinase, and activates the kinase. This activation leads to the phosphorylation of AgrA, which is linked to intergenic DNA between P2 and P3, thus leading to transcription activation. An increase in the transcription causes an increase in the intracellular concentrations of RNAIII, which is responsible for the translation of the secreted virulence factor; for example, *hla* encodes the α-toxin and reduces the expression of surface adhesins, such as protein A and fibronectin-binding protein [31]. Moreover, RNAIII stabilizes *mgrA* mRNA and increases a global transcriptional regulator called Mgr, which serves as an intermediate regulator for *agr* to function. The Mgr affect gene is involved in virulence processes, such as autolysis, antibiotic resistance, and biofilm formation [32].

The 4547-residue pro-AIP is synthesized by AgrD, and the 79-residue AIP is processed and secreted by the AgrB transporter. The pro-AIP is truncated and cyclized into a five-residue peptide by the action of a thiolactone link between the C-terminus and a cysteine residue. When there are additional bacteria, the AIP accumulates and binds to the Agr C membrane-bound histidine-kinase, thus activating the QS system. AgrA, the response regulator protein kinase, phosphorylates the conserved histidine and transfers the phosphate group to an aspartate residue. By attaching upstream of the P2 promotor, AgrA activates the feed-forward loop, leading to the expression of *agr* operon. The *hla* gene, which encodes for the virulence factor hemolysin, is expressed via the PIII promoter that is under the control of AgrA. On the one hand, RNAIII promotes the expression of toxins; on the other hand, it inhibits the activity of the rot factor, a repressor of toxins. The secretion of virulence factors and suppression of factors that control toxin synthesis are both outcomes of this QS regulatory cascade. Additionally, the QS system inhibits biofilm development in the HCD environment while regulating it in the LCD environment. As a result, the biofilm serves as a safe haven for the bacteria to continue multiplying until HCD is attained, after which they can move to other hosts [27].

Inactive *agr* confers an advantage to *S. aureus* to better adapt to and persist in the host cell. The *agr* system plays an important role in biofilm development, and *agr* mutants have a high tendency for biofilm formation. Cells disseminating from biofilms have exhibited active *agr* systems. Thus, the suppression of the *agr* system is required for biofilm formation. In this study, the mBTL (0.5 mg/mL) encapsulating ChNPs restricted *S. aureus* and MRSA biofilm formation by 51.7% and 50%, respectively. A greater reduction was observed in mutant strains with a significant ability for biofilm formation compared to the wild-type. The biofilm formation ability was reduced by 68% and 63.6% for the AgrA and AgrB mutants, respectively, and by 97.3% for the AgrC mutants, suggesting the potent inhibitory activity of mBTL-ChNPs [32].

In the current study, mBTL (0.5 mg/mL) encapsulating ChNPs decreased the biofilm formation ability of *S. aureus*, MRSA, and the AgrA and AgrB mutants by 51.7%, 50%, 68%, and 63.6%, respectively, and of AgrC by 97.3%. These results are consistent with

those of previous studies where chrysin-loaded ChNPs exhibited marked anti-biofilm activity against *S. aureus* compared to untreated bacteria [33]. Another study revealed that chitosan-coated iron oxide nanoparticles can successfully prevent bacterial colonization and reduce the development of biofilm in *S. aureus* by 53% [34]. The same results are shown in this study, and CLSM and SEM were used to visualize the antibiofilm activity of mBTL-loaded ChNPs against the tested bacterial isolates. These results indicate a decrease in the thickness and density of the biofilm matrix in the presence of NPs.

The biodegradability, biocompatibility, and low toxicity of chitosan have generated interest, and substantial research has been conducted on its potential uses in various industries. Some of the many potential applications of chitosan are as follows: hydrogel film in the pharmaceutical industry [35], flocking agent in wastewater treatment [25], plant defense elicitor [22], additive in food preservation [22], and drug delivery carrier [36,37]. Many studies have also revealed the broad antibacterial action of chitosan against bacteria and fungi. However, this action is very specific to the microorganism [38,39]. Furthermore, the physicochemical properties of chitosan are related to its antibacterial mechanism [40,41].

O'Loughlin et al. revealed that the effects of mBTL extend beyond those of an anti-infective agent. It can also reduce the formation of biofilms and the clogging of microfluidic devices. However, it has been suggested that using antiquorum-sensing molecules can prevent the failure of systems that are susceptible to fouling by biofilms [4]. As a result, these molecules may be used in other fields, including medicine. In this study, we administered the inhibitor in liquid form. We ultimately hope to include mBTL-like molecules in the list of materials used to manufacture such gadgets, making them inherently resistant to biofilms. Taken together, our results on mBTL provide strong evidence for the efficacy of quorum-sensing modulators in reducing pathogens with quorum-sensing-controlled phenotypes.

The results of the study by Eltayb et al. are in agreement with our results in terms of the effectiveness of loaded mBTL in decreasing the minimum inhibitory concentration of mBTL for different tested *Pseudomonas* isolates [42].

To the best of our knowledge, limited studies have investigated the effects of loaded mBTL on different bacterial strains, and most of these studies have been conducted on *Pseudomonas aeruginosa*. This makes ours a pioneer study on the effects of mBTL and loaded mBTL on different *Staphylococcus* strains. These promising results of loaded mBTL can be used as a reference for new generations of drugs to treat drug-resistant bacteria. This study has added to our knowledge on the MRSA virulence factors expression and a potential strategy to inhibit those factors using an anti-virulence agent.

5. Conclusions

The inhibition of quorum sensing is widely recognized as an effective antivirulence approach. We developed mBTL-loaded chitosan nanoparticles, which provided enhanced antibacterial activity against multiple staphylococcal strains compared to mBTL alone. The mBTL-ChNPs also reduced biofilm formation, as shown by crystal violet staining, CLSM, and SEM. The findings of this study suggest the potential therapeutic utility of mBTL-ChNPs in the treatment of *S. aureus* infection and the prevention of biofilm formation.

Author Contributions: F.S.A., F.Y.A. and R.A.: Conceptualization, design of study, methodology, acquisition of data, validation, supervision, resources, visualization, and writing—final draft preparation. E.K.E., B.M.A. and A.A.: Acquisition of data, analysis of data, visualization, interpretation of data, and writing—first draft preparation. H.A.: Chemical synthesis and analysis of mBTL and interpretation of all chemical analysis. E.E.: Nanoparticle formulation and analysis. S.H. and N.A.A.: Interpretation of data and writing—first draft. T.A.A.: Validation, resources, visualization, and writing—final draft preparation. All authors have read and agreed to the published version of the manuscript.

Funding: This research project was supported by the Researchers Supporting Project number (RSP2023340), King Saud University, Riyadh, Saudi Arabia.

Institutional Review Board Statement: Not applicable.

Informed Consent Statement: Not applicable.

Data Availability Statement: The data presented in this study are available upon request from the corresponding author.

Acknowledgments: All authors extend their sincere appreciation to the Researchers Supporting Project number (RSP2023340), King Saud University, Riyadh, Saudi Arabia.

Conflicts of Interest: The authors declare no conflict of interest.

References

1. Al Bshabshe, A.; Joseph, M.R.P.; Awad El-Gied, A.A.; Fadul, A.N.; Chandramoorthy, H.C.; Hamid, M.E. Clinical relevance and antimicrobial profiling of methicillin-resistant *Staphylococcus aureus* (mrsa) on routine antibiotics and ethanol extract of mango kernel. *BioMed Res. Int.* **2020**, *2020*, 415068. [CrossRef] [PubMed]
2. Nielsen, A.; Månsson, M.; Bojer, M.S.; Gram, L.; Larsen, T.; Novick, R.; Frees, D.; Frøkiær, H.; Ingmer, H. Solonamide B Inhibits quorum sensing and reduces *Staphylococcus aureus* mediated killing of human neutrophils. *PLoS ONE* **2014**, *9*, e84992. [CrossRef] [PubMed]
3. Choudhary, K.S.; Mih, N.; Monk, J.; Kavvas, E.; Yurkovich, J.T.; Sakoulas, G.P.B. The *Staphylococcus aureus* two-component system AgrAC displays four distinct genomic arrangements that delineate genomic virulence factor signatures. *Front. Microbiol.* **2022**, *9*, 1082. [CrossRef] [PubMed]
4. O'Loughlin, C.T.; Miller, L.C.; Siryaporn, A.; Drescher, K.; Semmelhack, M.F.; Bassler, B.L. A quorum-sensing inhibitor blocks *Pseudomonas aeruginosa* virulence and biofilm formation. *Proc. Natl. Acad. Sci. USA* **2013**, *110*, 17981–17986. [CrossRef]
5. Nguyen, H.M.; Graber, C.J. Limitations of antibiotic options for invasive infections caused by methicillin-resistant *Staphylococcus aureus*: Is combination therapy the answer. *J. Antimicrob. Chemother.* **2010**, *65*, 24–36. [CrossRef]
6. Alshamsan, A.; Aleanizy, F.S.; Badran, M.; Alqahtani, F.Y.; Alfassam, H.; Almalik, A.; Alosaimy, S. Exploring anti-MRSA activity of chitosan-coated liposomal dicloxacillin. *J. Microbiol. Methods* **2019**, *156*, 23–28. [CrossRef]
7. Wu, L.; Luo, Y. Bacterial quorum-sensing systems and their role in intestinal bacteria-host crosstalk. *Front. Microbiol.* **2021**, *12*, 611413. [CrossRef]
8. Zhang, J.; Feng, T.; Wang, J.; Wang, Y.; Zhang, X.H. The Mechanisms and Applications of Quorum Sensing (QS) and Quorum Quenching (QQ). *J. Ocean Univ. China* **2019**, *18*, 1427–1442. [CrossRef]
9. Reddy, C.A.; Beveridge, T.J.; Breznak, J.A.; Marzluf, G. *Methods for General and Molecular Microbiology*; American Society for Microbiology Press: Washington, DC, USA, 2007.
10. Burnside, K.; Lembo, A.; de Los Reyes, M.; Iliuk, A.; BinhTran, N.T.; Connelly, J.E.; Lin, W.J.; Schmidt, B.Z.; Richardson, A.R.; Fang, F.C.; et al. Regulation of hemolysin expression and virulence of *Staphylococcus aureus* by a serine/threonine kinase and phosphatase. *PLoS ONE* **2010**, *5*, e11071. [CrossRef]
11. Tal-Gan, Y.; Stacy, D.M.; Foegen, M.K.; Koenig, D.W.; Blackwell, H.E. Highly potent inhibitors of quorum sensing in *Staphylococcus aureus* revealed through a systematic synthetic study of the group-III autoinducing peptide. *J. Am. Chem. Soc.* **2013**, *135*, 7869–7882. [CrossRef]
12. Beceiro, A.; Tomás, M.; Bou, G. Antimicrobial resistance and virulence: A successful or deleterious association in the bacterial world? *Clin. Microbiol. Rev.* **2013**, *26*, 185–230. [CrossRef] [PubMed]
13. Zhao, D.; Yu, S.; Sun, B.; Gao, S.; Guo, S.; Zhao, K. Biomedical applications of chitosan and its derivative nanoparticles. *Polymers* **2018**, *10*, 462. [CrossRef] [PubMed]
14. Hoang, N.H.; Le Thanh, T.; Sangpueak, R.; Treekoon, J.; Saengchan, C.; Thepbandit, W.; Papathoti, N.K.; Kamkaew, A.; Buensanteai, N. Chitosan nanoparticles-based Ionic gelation method: A promising candidate for plant disease management. *Polymers* **2022**, *14*, 662. [CrossRef] [PubMed]
15. Marrie, T.; Costerton, J.W. Scanning and transmission electron microscopy of in situ bacterial colonization of intravenous and intraarterial catheters. *J. Clin. Microbiol.* **1984**, *19*, 687–693. [CrossRef]
16. Chikezie, I.O. Determination of minimum inhibitory concentration (MIC) and minimum bactericidal concentration (MBC) using a novel dilution tube method. *Afr. J. Microbiol. Res.* **2017**, *11*, 977–980. [CrossRef]
17. Eltayb, E.K.; Alqahtani, F.Y.; Alkahtani, H.M.; Alsarra, I.A.; Alfaraj, R.; Aleanizy, F.S. Attenuation of *Pseudomonas aeruginosa* quorum sensing virulence of biofilm and pyocyanin by mBTL-loaded calcium alginate nanoparticles. *Polymers* **2022**, *14*, 3655. [CrossRef]
18. Younes, I.; Rinaudo, M. Chitin and chitosan preparation from marine sources. Structure, properties and applications. *Mar. Drugs.* **2015**, *13*, 1133–1174. [CrossRef]
19. Xing, K.; Zhu, X.; Peng, X.; Qin, S. Chitosan antimicrobial and eliciting properties for pest control in agriculture: A review. *Agron. Sustain. Dev.* **2015**, *35*, 569–588. [CrossRef]
20. Bamm, V.V.; Ko, J.T.; Mainprize, I.L.; Sanderson, V.P.; Wills, M.K.B. Lyme disease frontiers: Reconciling borrelia biology and clinical conundrums. *Pathogens* **2019**, *8*, 299. [CrossRef]

21. Sharifi-Rad, J.; Quispe, C.; Butnariu, M.; Rotariu, L.S.; Sytar, O.; Sestito, S.; Rapposelli, S.; Akram, M.; Iqbal, M.; Krishna, A.; et al. Chitosan nanoparticles as a promising tool in nanomedicine with particular emphasis on oncological treatment. *Cancer Cell Int.* **2021**, *21*, 318. [CrossRef]
22. Herdiana, Y.; Wathoni, N.; Shamsuddin, S.; Muchtaridi, M. Drug release study of the Chitosan-based nanoparticles. *Heliyon* **2022**, *8*, e08674. [CrossRef] [PubMed]
23. Shi, S.F.; Jia, J.F.; Guo, X.K.; Zhao, Y.P.; Chen, D.S.; Guo, Y.Y.; Zhang, X.L. Reduced *Staphylococcus aureus* biofilm formation in the presence of chitosan-coated iron oxide nanoparticles. *Int. J. Nano Med.* **2016**, *11*, 6499–6506. [CrossRef] [PubMed]
24. Aleanizy, F.S.; Alqahtani, F.Y.; Shazly, G.; Alfaraj, R.; Alsarra, I.; Alshamsan, A.; Gareeb, A.; Hosam, G. Measurement and evaluation of the effects of pH gradients on the antimicrobial and antivirulence activities of chitosan nanoparticles in *Pseudomonas aeruginosa*. *Saudi Pharm. J.* **2018**, *26*, 79–83. [CrossRef]
25. Suligoy, C.M.; Lattar, S.M.; Noto Llana, M.; González, C.D.; Alvarez, L.P.; Robinson, D.A.; Gómez, M.I.; Buzzola, F.R.; Sordelli, D.O. Mutation of Agr is associated with the adaptation of Staphylococcus aureus to the host during chronic osteomyelitis. *Front. Cell. Infect. Microbiol.* **2018**, *8*, 18. [CrossRef] [PubMed]
26. Murray, E.J.; Crowley, R.C.; Truman, A.; Clarke, S.R.; Cottam, J.A.; Jadhav, G.P.; Steele, V.R.; O'Shea, P.; Lindholm, C.; Cockayne, A.; et al. Targeting Staphylococcus aureus quorum sensing with nonpeptidic small molecule inhibitors. *J. Med. Chem.* **2014**, *57*, 2813–2819. [CrossRef]
27. Mandal, S.M.; Ghosh, A.K.; Pati, B.R. Dissemination of antibiotic resistance in methicillin-resistant *Staphylococcus aureus* and vancomycin-resistant *S. aureus* strains isolated from hospital effluents. *Am. J. Infect. Control* **2015**, *43*, e87–e88. [CrossRef]
28. Novick, R.P. Autoinduction and signal transduction in the regulation of staphylococcal virulence. *Mol. Microbiol.* **2003**, *48*, 1429–1449. [CrossRef]
29. Boles, B.R.; Horswill, A.R. Agr-mediated dispersal of *Staphylococcus aureus* biofilms. *PLoS Pathog.* **2008**, *4*, e1000052. [CrossRef]
30. Yarwood, J.M.; Bartels, D.J.; Volper, E.M.; Greenberg, E.P. Quorum sensing in *Staphylococcus aureus* biofilms. *J. Bacteriol.* **2004**, *186*, 1838–1850. [CrossRef]
31. Gupta, R.K.; Luong, T.T.; Lee, C.Y. RNAIII of the *Staphylococcus aureus* agr system activates global regulator MgrA by stabilizing mRNA. *Proc. Natl. Acad. Sci. USA* **2015**, *112*, 14036–14041. [CrossRef]
32. Krismer, B.; Peschel, A. Does *Staphylococcus aureus* nasal colonization involve biofilm formation? *Future Microbiol.* **2011**, *6*, 489–493. [CrossRef] [PubMed]
33. Messias de Souza, G.; Gervasoni, L.F.; Rosa, R.D.S.; de Souza Iacia, M.V.M.; Nai, G.A.; Pereira, V.C.; Winkelströter, L.K. Quercetin-loaded chitosan nanoparticles as an alternative for controlling bacterial adhesion to urethral catheter. *Int. J. Urol.* **2022**, *29*, 1228–1234. [CrossRef]
34. Siddhardha, B.; Pandey, U.; Kaviyarasu, K.; Pala, R.; Syed, A.; Bahkali, A.H.; Elgorban, A.M. Chrysin-loaded chitosan nanoparticles potentiates antibiofilm activity against *Staphylococcus aureus*. *Pathogens* **2020**, *9*, 115. [CrossRef] [PubMed]
35. Abebe, L.S.; Chen, X.; Sobsey, M.D. Chitosan coagulation to improve microbial and turbidity removal by ceramic water filtration for household drinking water treatment. *Int. J. Environ. Res. Public Health* **2016**, *13*, 269. [CrossRef] [PubMed]
36. Diekema, D.J.; Richter, S.S.; Heilmann, K.P.; Dohrn, C.L.; Riahi, F.; Tendolkar, S.; McDanel, J.S.; Doern, G.V. Continued emergence of USA 300 methicillin-resistant *Staphylococcus aureus* in the United States: Results from a nationwide surveillance study. *Infect. Control Hosp. Epidemiol.* **2014**, *35*, 285–292. [CrossRef]
37. Alvarez Echazu, M.I.; Olivetti, C.E.; Anesini, C.; Perez, C.J.; Alvarez, G.S.; Desimone, M.F. Development and evaluation of thymol-chitosan hydrogels with antimicrobial-antioxidant activity for oral local delivery. *Mater. Sci. Eng. Mater. Biol. Appl.* **2017**, *81*, 588–596. [CrossRef]
38. Sharma, P.K.; Halder, M.; Srivastava, U.; Singh, Y. Antibacterial PEG-chitosan hydrogels for controlled antibiotic/protein delivery. *ACS Appl. Bio Mater.* **2019**, *2*, 5313–5322. [CrossRef]
39. Li, B.; Shan, C.L.; Ge, M.Y.; Wang, L.; Fang, Y.; Wang, Y.L.; Xie, G.L.; Sun, G.C. Antibacterial mechanism of chitosan and its applications in protection of plant from bacterial disease. *Asian J. Chem.* **2013**, *25*, 10033–10036. [CrossRef]
40. Varlamov, V.P.; Mysyakina, I.S. Chitosan in biology, microbiology, medicine, and agriculture. *Microbiology* **2018**, *87*, 712–715. [CrossRef]
41. Rabea, E.I.; Badawy, M.E.T.; Stevens, C.V.; Smagghe, G.; Steurbaut, W. Chitosan as antimicrobial agent: Applications and mode of action. *Biomacromolecules* **2003**, *4*, 1457–1465. [CrossRef]
42. Khan, S.; Tøndervik, A.; Sletta, H.; Klinkenberg, G.; Emanuel, C.; Onsøyen, E.; Myrvold, R.; Howe, R.A.; Walsh, T.R.; Hill, K.E.; et al. Overcoming drug resistance with alginate oligosaccharides able to potentiate the action of selected antibiotics. *Antimicrob. Agents Chemother.* **2012**, *56*, 5134–5141. [CrossRef] [PubMed]